The GALAH survey: a new constraint on cosmological lithium and Galactic lithium evolution from warm dwarf stars

Xudong Gao [1]⋆†, Karin Lind,[1,2]⋆ Anish M. Amarsi [1,3], Sven Buder [1,4,5]†
Joss Bland-Hawthorn [5,6] Simon W. Campbell,[7] Martin Asplund,[4,5]
Andrew R. Casey [7,8] Gayandhi M. De Silva,[5,9] Ken C. Freeman,[4]
Michael R. Hayden,[5,6] Geraint F. Lewis [6] Sarah L. Martell [5,10],
Jeffrey D. Simpson [10], Sanjib Sharma [5,6], Daniel B. Zucker,[5,11,12] Tomaž Zwitter [13],
Jonathan Horner,[14] Ulisse Munari,[15] Thomas Nordlander [4,5] Dennis Stello,[5,10,16]
Yuan-Sen Ting,[4,17,18,19] Gregor Traven,[20] Robert A. Wittenmyer[21] and
the GALAH Collaboration

Affiliations are listed at the end of the paper

ABSTRACT

Lithium depletion and enrichment in the cosmos is not yet well understood. To help tighten constraints on stellar and Galactic evolution models, we present the largest high-resolution analysis of Li abundances A(Li) to date, with results for over 100 000 GALAH (Galactic Archeology with HERMES) field stars spanning effective temperatures 5900 K $\lesssim T_{\rm eff} \lesssim$ 7000 K and metallicities $-3 \lesssim$ [Fe/H] $\lesssim +0.5$. We separated these stars into two groups, on the warm and cool sides of the so-called Li dip, a localized region of the Kiel diagram wherein lithium is severely depleted. We discovered that stars in these two groups show similar trends in the A(Li)–[Fe/H] plane, but with a roughly constant offset in A(Li) of 0.4 dex, the warm group having higher Li abundances. At [Fe/H] $\gtrsim -0.5$, a significant increase in Li abundance with increasing metallicity is evident in both groups, signalling the onset of significant Galactic production. At lower metallicity, stars in the cool group sit on the Spite plateau, showing a reduced lithium of around 0.4 dex relative to the primordial value predicted from big bang nucleosynthesis (BBN). However, stars in the warm group between [Fe/H] $= -1.0$ and -0.5 form an elevated plateau that is largely consistent with the BBN prediction. This may indicate that these stars in fact preserve the primordial Li produced in the early Universe.

Key words: techniques: spectroscopic – stars: abundances – stars: atmospheres – stars: late-type – Galaxy: abundances – cosmology: primordial nucleosynthesis.

1 INTRODUCTION

Lithium is a fragile element that can be destroyed by proton capture reactions at relatively low temperatures ($\sim 2.5 \times 10^6$ K) in stellar interiors (Pinsonneault 1997). Standard stellar evolution models suggest that the convective envelopes are weakly developed in low-mass unevolved (main-sequence) stars with effective temperatures ($T_{\rm eff}$) larger than 6000 K, thus precluding the surface Li from reach-

ing the interior to be destroyed (Deliyannis, Demarque & Kawaler 1990). As such, the unevolved, metal-poor stars are expected to retain near-primordial Li abundances, providing an opportunity to put constraints on big bang nucleosynthesis (BBN). However, a significant difference has been found between the Li abundance measured from very metal-poor stars in the Galaxy that fall on the so-called Spite plateau at A(Li)[1] $\approx$ 2.2 (Spite & Spite 1982) and the prediction by standard BBN models, A(Li) $= 2.75 \pm 0.02$ (Pitrou et al. 2018). This is the well-known cosmological lithium problem

---

[1]A(Li) $= \log{(n_{\rm Li}/n_{\rm H})} + 12$, where $n_{\rm Li}$ and $n_{\rm H}$ are the the number densities of lithium and hydrogen, respectively.

(Spite, Spite & Bonifacio 2012). It has been suggested that the metal-poor stars we observe have undergone lithium depletion by an amount that may be quantified by comparing stellar abundances to evolutionary models with atomic diffusion and an unknown source of mixing in the stellar interior (Richard, Michaud & Richer 2005; Korn et al. 2006). The results do alleviate the tension to standard big bang, but may do not fully bridge the gap as initial abundances of the order of ~2.57 (Nordlander et al. 2012) or ~2.46 (Mucciarelli, Salaris & Bonifacio 2012) are inferred.

A striking feature called the 'lithium dip' (Li dip) was first observed in (Population I) main-sequence stars in the Hyades open cluster by Wallerstein, Herbig & Conti (1965), and confirmed by later studies (Boesgaard & Tripicco 1986; Burkhart & Coupry 2000; Boesgaard et al. 2016). Li abundances show a significant drop in the temperature range of 6400–6850 K. Within this narrow temperature range, the depletion in A(Li) can reach a factor of 100 relative to stars out of this region. On the warm side of the Li dip, the Li abundances increase sharply with increasing effective temperature. For T_{eff} larger than ~6900 K, the Li abundances seem to remain constant, compatible with the Galactic value (i.e. the meteoritic value; see Lodders, Palme & Gail 2009). However, few abundance determinations are available for stars in this T_{eff} region, because the primary abundance diagnostic, the Li I 670.8 nm resonance line, is weaker in warmer stars; excessive line broadening due to typically fast stellar rotation further complicates spectroscopic analyses. On the cool side of the Li dip, the Li abundances increase gradually with decreasing effective temperature until reaching a sort of plateau, which extends from ~6400 to ~6000 K. Stars in this region are slightly depleted in lithium; however, this depletion is uniform, and is not nearly as severe as in the Li-dip stars.

Since the first observations, the presence of the Li dip has also been found in many older star clusters, such as NGC 752 and M67 (Balachandran 1995), but not in the youngest open clusters (Boesgaard, Budge & Ramsay 1988; Balachandran, Mallik & Lambert 2011) – those with ages less than about 100 Myr. This indicates that the large lithium depletions that are now apparent in the Li dip take place when the stars are on the main sequence, rather than being there from the star's birth, or occurring when the star was on the pre-main-sequence phase.

In order to meet observational constraints such as the complicated Li abundance behaviour observed in the main-sequence stars, several different non-standard stellar evolution models have been proposed, which take into consideration atomic diffusion (Michaud 1986) and rotation-induced mixing (Zahn 1992). However, these models cannot accurately account for the observed Li dip. More recent works successfully managed to describe the Li dip in young stellar cluster Hyades by also accounting for internal gravity waves (Montalbán & Schatzman 2000; Charbonnel & Talon 2005). According to their models, one can describe the Li-dip feature by characterizing the stars into three groups based on temperature (Charbonnel & Talon 2005): those warmer than the Li dip, those within the Li dip, and those cooler. Stars in the warm group have the shallowest convective envelopes, making them nearly unaffected by diffusion and rotation-induced mixing. Li-dip stars experience rotational mixing as the convective envelope deepens, resulting in severe Li destruction. However, for stars in the cool group, even though they have even deeper convective envelopes, internal gravity waves become activated and efficiently extract angular momentum from the interior; this counteracts the rotational mixing, and limits the amount of lithium destruction. For these reasons, stars on either side of the Li dip have mechanisms to prevent lithium destruction

to different extents. In particular, the warm stars may allow us to probe the primordial Li abundance.

The Li-dip phenomenon has also been observed in unevolved field stars (e.g. Randich et al. 1999; Chen et al. 2001; Lambert & Reddy 2004; Ramírez et al. 2012; Aguilera-Gómez, Ramírez & Chanamé 2018; Bensby & Lind 2018). These earlier studies have typical sample sizes of 200–2000 field stars in total, thus spanning only very limited ranges in stellar properties and containing very few stars on the warm side of the Li dip. To study the lithium evolution comprehensively, a large sample of stars with homogeneous measurements is needed.

The aim of this paper is to investigate the behaviour of lithium among late-type field stars, including main-sequence, turn-off, and early subgiant phase. Using data from the Galactic Archeology with HERMES (GALAH) survey (De Silva et al. 2015), we present the largest sample of lithium abundances so far. The data span benefit from a homogeneous determination of stellar parameters and lithium abundances, and span a wide range of metallicities. These two aspects of our study allow us to draw fresh insights into the lithium puzzle.

2 OBSERVATIONS AND ANALYSIS

We observed over 650 000 FGK field stars in the solar neighbourhood as part of the GALAH (De Silva et al. 2015), K2-HERMES (Sharma et al. 2019), and TESS–HERMES (Sharma et al. 2018) spectroscopic surveys. The spectral resolving power of the surveys $R = \lambda/\Delta\lambda \approx 28\,000$ is sufficiently matched to the stellar absorption lines under study. To avoid stars with large convection-driven lithium depletion, we mainly target the dwarf and subgiant stars with T_{eff} ranging from 5900 to 7000 K covering a large range of metallicity from [Fe/H] = +0.5 to [Fe/H] = −3.0, which includes the Spite plateau at the metal-poor end. After excluding spectroscopically resolved binaries, and observations with fitting inaccuracies, low signal-to-noise ratio, strong emission lines, or reduction issues, we obtain a set of 62 945 stars with lithium detections and a separate set of 59 117 stars with upper limits on the Li abundance.

The stellar parameters T_{eff}, [Fe/H], projected rotational velocities $v\sin\iota$, and line-of-sight radial velocity were determined simultaneously in a homogeneous way by fitting observed neutral and ionized lines of Sc, Ti, and Fe lines that are unblended and for which reliable atomic data are available, as well as the T_{eff}-sensitive Hα and Hβ lines, using the GALAH analysis pipeline (Buder et al. 2018). Surface gravities were constrained consistently and simultaneously by the fundamental relation between the absolute magnitude, mass, and T_{eff} (Buder et al. 2019). Stellar masses and ages were estimated by a Bayesian implementation of isochrone fitting (Lin et al. 2018). Having obtained the optimal stellar parameters, Li abundances were then derived using non-local thermodynamic equilibrium spectral synthesis (Gao et al. 2018) for the Li I 670.8 nm resonance line. The non-LTE departure coefficients come from the model described in Lind, Asplund & Barklem (2009).

In this work, we consider lithium to be detected when the line depression (i.e. $D \equiv 1 - F_{\lambda}/F_c$) is deeper than 1.5σ of the flux error within the line mask, and at least 3 per cent below the normalized continuum flux. In all other cases, the measurement is considered as an upper limit. We estimate upper limits on the Li abundance based on linear interpolation in four dimensions, using a large matrix that connects line strength with Li abundance, effective temperature, surface gravity, and rotational velocity.

3 RESULTS

Fig. 1 shows the locations of the sample stars with lithium detections and upper limits in the Kiel diagram, respectively. Comparing the two panels, a clear gap is seen in the distribution of stars for which lithium could be detected (Fig. 1b), whereas a significant overdensity of stars for which only upper limits on the Li abundance could be obtained is seen in the same region (Fig. 1a). Most of the stars with upper limits are concentrated in this diagonal region between $T_{eff} \sim 6300$ and 6600 K, with surface gravity (log g) ranging from 3.8 to 4.3 dex. We interpret this as the Li-dip region: these stars have experienced severe lithium depletion and are now evolving towards the subgiant branch.

To characterize the Li-dip region in the Kiel diagram, we first narrow down the log g range of our sample (3.7−4.5 dex) to reduce the evolutionary effects on lithium due to post-main-sequence stars. Our sample now consists of upper main-sequence stars, turn-off stars, and early subgiants. Moreover, we remove all the stars with T_{eff} less than 6000 K, as those cooler stars undergo strong and rapid lithium depletion, due to their larger convective envelopes (e.g. Bensby & Lind 2018). The density contours are then overplotted on the distribution of A(Li) upper limits. We define the approximate boundaries of the Li-dip region by using linear fits in the left and right edges of the outermost contour. We delineate the left and right boundaries of the Li-dip region as the warm group and cool group of stars, respectively.

The left-hand panel of Fig. 2 shows lithium trends as a function of metallicity, for the warm and cool groups of stars. At low metallicity ([Fe/H] $\lesssim -1$ dex), the stars in the cool group have ages in excess of 11 Gyr and reveal the Spite plateau, showing low and near-constant Li abundances. In contrast, there are no old, metal-poor warm stars in our sample: such stars have higher masses and have evolved off the main sequence after such a long period. Thus, the stars in the warm group only appear above [Fe/H] $\gtrsim -1.0$. Up to $-1.0 \lesssim$ [Fe/H] $\lesssim -0.5$, the warm group having 117 stars shows a similar constant lithium plateau, but elevated by almost three times that of the cool group (0.4 dex). We measure A(Li) = 2.69 ± 0.06. Remarkably, this plateau is largely consistent with the predictions of BBN [A(Li) = 2.75 ± 0.02]. One interpretation of this is that both Galactic enrichment and stellar destruction have been insignificant in this population of stars; in other words, these stars in fact may preserve the primordial Li produced in the early Universe.

At higher metallicities [Fe/H] $\gtrsim -0.5$, both the warm and cool groups of stars show an increasing trend in A(Li). This is probably caused by Galactic enrichment (Prantzos et al. 2017). It is interesting to note that even in this metallicity regime, the difference in the average Li abundances between the warm and cool groups is still 0.4 dex, and remains so up to solar metallicity.

The right-hand panel of Fig. 2 shows the corresponding location of warm and cool group stars in the Kiel diagram with colour-coded Li abundances. There is a clear gradient in the Li abundances across the Kiel diagram, delineating the Li dip from the warm and cool groups of stars. It shows that stars in the cool group are systematically more depleted in lithium than those in the warm group. Since most of our stars are centred around the solar metallicity, we overplotted the evolutionary tracks of different masses in solar metallicity on the distribution of our targets. The theoretical models support our speculation that we have captured the evolutionary track of Li-dip stars in our observations.

At a given [Fe/H], there is a difference in mean age between the warm group (young) and cool group (old), because of the sample

selection method. The age difference is largest at low metallicity (up to 7 Gyr) and steadily decreases to become insignificant at the highest metallicities. The lower Li abundances of the cool group should thus be interpreted as a combined effect of their lower effective temperatures and older ages, making depletion more efficient and giving it longer time to act. Sestito & Randich (2005) carried out a detailed investigation of lithium depletion time-scales in late-type stars at this temperature with metallicities $-0.2 \lesssim$ [Fe/H] $\lesssim +0.2$. They found that main-sequence lithium depletion is not a continuous process and becomes ineffective beyond an age of 1–2 Gyr for the majority of stars, leading to a Li plateau at older ages. The total amount of lithium depletion during the main-sequence lifetime is around 0.5 dex.

The age difference between the warm and cool groups may lead one to speculate that Galactic chemical evolution has elevated the initial Li abundances in the warm group compared to those in the cool group. However, our data suggest that such enrichment scales with increasing metallicity and only becomes noticeable at [Fe/H] $\gtrsim -0.5$, where Fig. 2 shows the stars in both the warm and cool groups clearly rise off their respective plateaus. Moreover, recent observations of Li abundances in the low-metallicity gas ([Fe/H] ≈ -0.5) of the Small Magellanic Cloud (Howk et al. 2012) and in warmer stars in the open cluster NGC 2243 (François et al. 2013) ([Fe/H] = -0.52; an estimated age of 4.3 Gyr) are in good agreement with mean A(Li) measurements in the warm plateau stars. The values of Li abundance obtained from these observations are all comparable to the primordial Li abundance predicted by BBN.

4 CONCLUSIONS

To reduce the complex behaviour of lithium in the field stars, for the first time we draw a comparison between the warm and cool groups of stars, which are located on the warm and cool sides of the Li dip, respectively. Here, we find that Li abundances in the two groups show a similar pattern as a function of [Fe/H]; however, stars in the cool group are more depleted in lithium than those in the warm group by a factor of 3. This difference is determined from more than 100 000 stars that have a wide range of stellar properties and chemistry. The implications we can obtain from this result are as follows:

(i) We find that at $-1.0 \lesssim$ [Fe/H] $\lesssim -0.5$, the average Li abundance of stars warmer than the Li dip shows an elevated lithium plateau, the value of which is consistent with the primordial Li abundance as predicted by BBN within the errors. Since Galactic production of lithium has not yet contributed significantly to the cooler Spite plateau in this metallicity regime, we suggest that the Li abundance measured in the warm group is indicative of insignificant Li depletion as well as insignificant Li enrichment in these stars. This interpretation would explain why the Li abundances closely resemble the BBN primordial value, and is consistent with what has been reported for the Small Magellanic Cloud (Howk et al. 2012) and in the open cluster NGC 2243 (François et al. 2013). Regardless of the possibility that minor depletion and enrichment may have cancelled each other out in this group of stars, the values provide a valuable constraint on both cosmological models of the early universe and stellar evolution models.

(ii) We infer that, at a given metallicity, the three different regimes (warm, Li dip, and cool) follow different lithium depletion mechanisms. For the stars in the cool group, the depletion is not strongly dependent on metallicity; instead, it is primarily governed by a star's main-sequence temperature and age. How much lithium
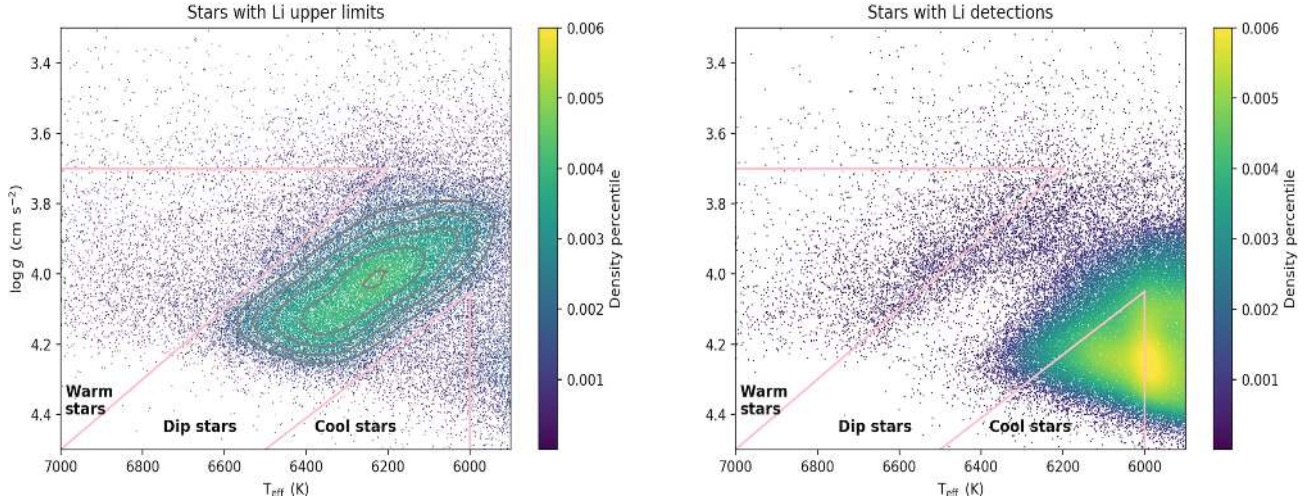
Figure 1. Loci of the sample stars with A(Li) upper limits and lithium detections in the T_{eff}–$\log g$ panel, respectively. *Left-hand panel*: Loci of stars with lithium upper limits (62 945 stars). The colour bar represents density distribution of stars, with bright colours implying high density. The contours that are overplotted represent the density percentile of lithium upper limit stars. We define the approximate boundaries of the Li-dip region by using linear fits in the left and right edges of the outermost contour. The boxes that are located inside the pink triangles are classified as the warm group and cool group of stars, respectively. Stars that lie outside these three regions are removed from the comparison in Fig. 2. *Right-hand panel*: Loci of stars with lithium detections (59 117 stars).
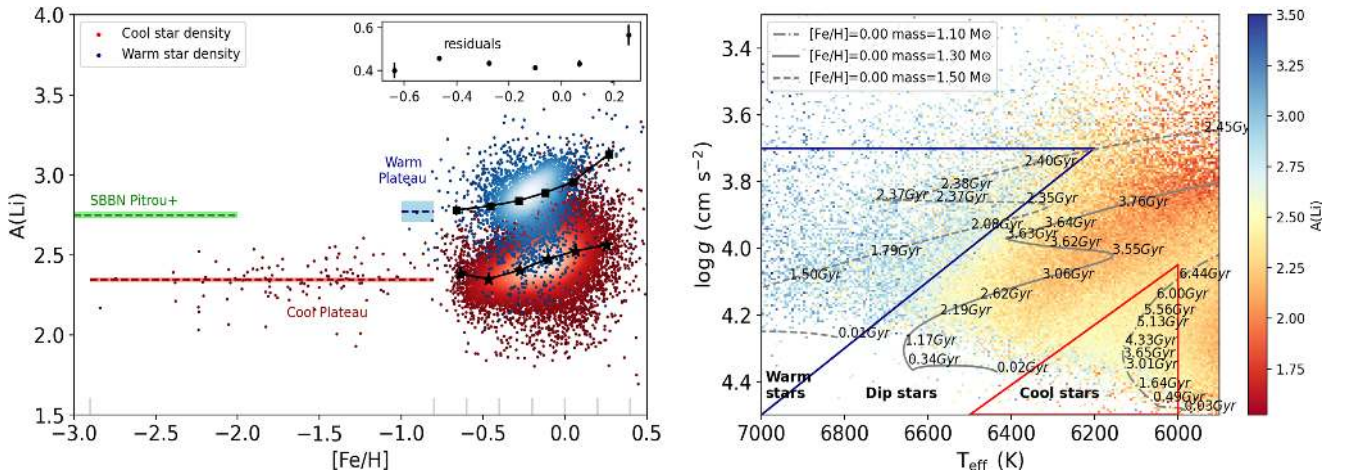
Figure 2. Lithium trends as a function of metallicity as observed for the warm and cool groups of stars. *Left-hand panel*: Observational data of lithium from the warm and cool groups as a function of [Fe/H]. Only detections are retained in each group and plotted as colour-coded density. Black squares and asterisks represent the median Li abundances of the metallicity bins in the warm and cool groups of stars, respectively. The corresponding metallicity bin sizes are indicated with grey lines above the bottom axis. The error bars represent the uncertainties of the mean; most of them are too small to be shown. The residual of the mean Li abundances between the two groups in the corresponding metallicity range is shown as an inset in the upper right corner. The mean values of stars in the most metal-poor bin that stretches between $-2.9 <$ [Fe/H] < -0.8 are instead marked with blue and red dashed lines for the warm and cool groups of stars, respectively, and marked as 'warm plateau' (six stars) and 'cool plateau' (108 stars). The corresponding shaded areas represent the standard error of the mean. The primordial Li abundance from the standard BBN (Pitrou et al. 2018) is shown with a green dashed line, which is in close agreement with the warm plateau within the errors. *Right-hand panel*: All the stars with lithium detections and upper limits are colour coded by A(Li) in the T_{eff}–$\log g$ panel. The corresponding locations of the warm and cool groups of stars are shown in the blue and red boxes, respectively. The colour gradient of Li abundance clearly shows the lithium differences between the three regions. Evolutionary tracks of different masses in the solar metallicity are overplotted.

has been depleted is a combination of temperature and stellar age, causing a near-constant offset with respect to the warm group.

(iii) We identify [Fe/H] ≈ -0.5 as the turning point where the Li abundances break the plateau and Galactic lithium production becomes significant. We see this in both the warm and the cool groups of stars. Given that the Spite plateau stars (of the cool group) have already experienced a large depletion of lithium and therefore do not reflect the true primordial value, we recommend that modellers apply the BBN-predicted Li abundance, instead of

the Spite plateau (Spite & Spite 1982) Li abundance, as the initial value in chemical evolution models (Prantzos 2012; Prantzos et al. 2017).

ACKNOWLEDGEMENTS

REFERENCES

Aguilera-Gómez C., Ramírez I., Chanamé J., 2018, A&A, 614, A55
Balachandran S., 1995, ApJ, 446, 203
Balachandran S. C., Mallik S. V., Lambert D. L., 2011, MNRAS, 410, 2526
Bensby T., Lind K., 2018, A&A, 615, A151
Boesgaard A. M., Tripicco M. J., 1986, ApJ, 302, L49
Boesgaard A. M., Budge K. G., Ramsay M. E., 1988, ApJ, 327, 389
Boesgaard A. M., Lum M. G., Deliyannis C. P., King J. R., Pinsonneault M. H., Somers G., 2016, ApJ, 830, 49
Buder S. et al., 2018, MNRAS, 478, 4513
Buder S. et al., 2019, A&A, 624, A19
Burkhart C., Coupry M. F., 2000, A&A, 354, 216
Charbonnel C., Talon S., 2005, in Alecian G., Richard O., Vauclair S., eds, EAS Publ. Ser. Vol. 17, Element Stratification in Stars: 40 Years of Atomic Diffusion, EDP Sciences, France. p. 167
Chen Y. Q., Nissen P. E., Benoni T., Zhao G., 2001, A&A, 371, 943
Deliyannis C. P., Demarque P., Kawaler S. D., 1990, ApJS, 73, 21
De Silva G. M. et al., 2015, MNRAS, 449, 2604
François P., Pasquini L., Biazzo K., Bonifacio P., Palsa R., 2013, A&A, 552, A136
Gao X. et al., 2018, MNRAS, 481, 2666
Howk J. C., Lehner N., Fields B. D., Mathews G. J., 2012, Nature, 489, 121
Korn A. J., Grundahl F., Richard O., Barklem P. S., Mashonkina L., Collet R., Piskunov N., Gustafsson B., 2006, Nature, 442, 657
Lambert D. L., Reddy B. E., 2004, MNRAS, 349, 757
Lin J., Dotter A., Ting Y.-S., Asplund M., 2018, MNRAS, 477, 2966
Lind K., Asplund M., Barklem P. S., 2009, A&A, 503, 541
Lodders K., Palme H., Gail H.-P., 2009, Landolt Börnstein, 4B, 560
Michaud G., 1986, ApJ, 302, 650
Montalbán J., Schatzman E., 2000, A&A, 354, 943
Mucciarelli A., Salaris M., Bonifacio P., 2012, MNRAS, 419, 2195
Nordlander T., Korn A. J., Richard O., Lind K., 2012, ApJ, 753, 48
Pinsonneault M., 1997, ARA&A, 35, 557
Pitrou C., Coc A., Uzan J.-P., Vangioni E., 2018, Phys. Rep., 754, 1
Prantzos N., 2012, A&A, 542, A67
Prantzos N., de Laverny P., Guiglion G., Recio-Blanco A., Worley C. C., 2017, A&A, 606, A132
Ramírez I., Fish J. R., Lambert D. L., Allende Prieto C., 2012, ApJ, 756, 46
Randich S., Gratton R., Pallavicini R., Pasquini L., Carretta E., 1999, A&A, 348, 487
Richard O., Michaud G., Richer J., 2005, ApJ, 619, 538
Sestito P., Randich S., 2005, A&A, 442, 615
Sharma S. et al., 2018, MNRAS, 473, 2004
Sharma S. et al., 2019, MNRAS, 490, 5335
Spite F., Spite M., 1982, A&A, 115, 357
Spite M., Spite F., Bonifacio P., 2012, Mem. Soc. Astron. Ital. Suppl., 22, 9
Wallerstein G., Herbig G. H., Conti P. S., 1965, ApJ, 141, 610
Zahn J.-P., 1992, A&A, 265, 115

[1]*Max-Planck-Institut für Astronomie (MPIA), Königstuhl 17, D-69117 Heidelberg, Germany*
[2]*Department of Astronomy, Stockholm University, AlbaNova, Roslagstullbacken 21, SE-10691 Stockholm, Sweden*
[3]*Theoretical Astrophysics, Department of Physics and Astronomy, Uppsala University, Box 516, SE-751 20 Uppsala, Sweden*
[4]*Research School of Astronomy & Astrophysics, Australian National University, Canberra, ACT 2611, Australia*
[5]*Center of Excellence for All Sky Astrophysics in Three Dimensions (ASTRO-3D),ACT 2611, Australia*
[6]*Sydney Institute for Astronomy (SIfA), School of Physics (A28), The University of Sydney, Sydney, NSW 2006, Australia*
[7]*School of Physics and Astronomy, Monash University, Clayton, VIC 3800, Australia*
[8]*Monash Centre for Astrophysics, Monash University, Clayton, VIC 3800, Australia*
[9]*Australian Astronomical Optics, Macquarie University, 105 Delhi Rd, North Ryde, NSW 2113, Australia*
[10]*School of Physics, University of New South Wales, Sydney, NSW 2052, Australia*
[11]*Department of Physics and Astronomy, Macquarie University, Sydney, NSW 2109, Australia*
[12]*Macquarie University Research Centre for Astronomy, Astrophysics & Astrophotonics, Sydney, NSW 2109, Australia*
[13]*Faculty of Mathematics and Physics, University of Ljubljana, Jadranska 19, 1000 Ljubljana, Slovenia*
[14]*University of Southern Queensland, Centre for Astrophysics, Toowoomba, QLD 4350, Australia*
[15]*INAF Astronomical Observatory of Padova, I-36012 Asiago, Italy*
[16]*Stellar Astrophysics Centre, Department of Physics and Astronomy, Aarhus University, DK-8000 Aarhus C, Denmark*
[17]*Institute for Advanced Study, Princeton, NJ 08540, USA*
[18]*Department of Astrophysical Sciences, Princeton University, Princeton, NJ 08544, USA*
[19]*Observatories of the Carnegie Institution of Washington, 813 Santa Barbara Street, Pasadena, CA 91101, USA*
[20]*Lund Observatory, Department of Astronomy and Theoretical Physics, Lund University, Box 43, SE-221 00 Lund, Sweden*
[21]*Computational Engineering and Science Research Centre, University of Southern Queensland, Toowoomba, QLD 4350, Australia*

This paper has been typeset from a TEX/LATEX file prepared by the author.